Journal of Biomechanics 96 (2019) 109349

Contents lists available at ScienceDirect

Journal of Biomechanics

journal homepage: www.elsevier.com/locate/jbiomech
www.JBiomech.com

Predictive regression modeling of body segment parameters using individual-based anthropometric measurements

Zachary Merrill [a,*], Subashan Perera [b,c], Rakié Cham [a,d,e]

[a] Department of Bioengineering, University of Pittsburgh, Pittsburgh, PA, USA
[b] Department of Medicine, University of Pittsburgh, Pittsburgh, PA, USA
[c] Department of Biostatistics, University of Pittsburgh, PA, USA
[d] Department of Physical Therapy, University of Pittsburgh, Pittsburgh, PA, USA
[e] Department of Ophthalmology, University of Pittsburgh, Pittsburgh, PA, USA

ARTICLE INFO

Article history:
Accepted 16 September 2019

Keywords:
Age
Body mass index
Anthropometry
Body segment parameters

ABSTRACT

Body segment parameters such as segment mass, center of mass, and radius of gyration are used as inputs in static and dynamic ergonomic and biomechanical models used to predict joint and muscle forces, and to assess risks of musculoskeletal injury. Previous work has predicted body segment parameters (BSPs) in the general population using age and obesity levels as statistical predictors (Merrill et al., 2017). Estimated errors in the prediction of BSPs can be as large as 40%, depending on age, and the prediction method employed (Durkin and Dowling, 2003). Thus, more accurate and representative segment parameter inputs are required for attempting to predict modeling outputs such as joint contact forces, muscle forces, and injury risk in individuals. This study aims to provide statistical models for predicting torso, thigh, shank, upper arm, and forearm segment parameters in working adults using whole body dual energy x-ray absorptiometry (DXA) scan data along with a set of anthropometric measurements. The statistical models were developed on a training data set, and independently validated on a separate test data set. The predicted BSPs in validation data were, on average, within 5% of the actual in vivo DXA-based BSPs, while previously developed predictions (de Leva, 1996) had average errors of up to 60%, indicating that the new models greatly increase the accuracy in predicting segment parameters. These final developed models can be used for calculating representative BSPs in individuals for use in modeling applications dependent on these parameters.

1. Introduction

Body segment parameters (BSPs), which include the length, segment mass, center of mass (COM), and radius of gyration (R_G) of body parts, are used in human factors and ergonomics, as well as biomechanical modeling applications. These applications include the design of tools, protective clothing, equipment, and workstations (Chaffin et al., 2006) based on segment size and ranges of motion, while static models such as the 3D Static Strength Prediction Model are dependent on segment position, length, mass, and COM inputs (Chaffin and Muzaffer, 1991). Inverse dynamics models use these segment position, length, and mass inputs, in addition to the segment inertial properties and dynamic data in order to determine joint contact forces and moments, along with the related injury risk in individuals during a specified task.

Previously developed approaches used to estimate BSPs are discussed in detail in Merrill et al (2019), including the limitations of these methodologies. For brevity purposes, only a summary is provided here. These BSP estimation approaches include regression equations from cadaver data (Chandler et al., 1975; Dempster, 1955), imaging techniques (de Leva, 1996), geometric modeling of the body (Pavol et al., 2002), inverse dynamics analyses (Hansen et al., 2014), static force plate analyses (Chen et al., 2011; Damavandi et al., 2009) and photographic analysis (Jensen, 1978; Sanders et al., 2015). Methods have also been developed utilizing individual anthropometric measurements in order to predict whole body COM position (Erdmann and Kowalczyk, 2015), as well as BSPs of all major body parts (Hatze, 1980).

The accuracy of the estimated BSPs can significantly impact the validity of biomechanical tools needing these sets of anthropometric data. For example, inverse dynamics models related to lifting

* Corresponding author at: Department of Bioengineering, 301 Schenley Place, 4420 Bayard St., Pittsburgh, PA 15213, USA.
E-mail address: zfm1@pitt.edu (Z. Merrill).

https://doi.org/10.1016/j.jbiomech.2019.109349
0021-9290/

and associated injury risk have been shown to be sensitive to errors in estimated COM position, joint rotation center location, length, and segment mass values (de Looze et al., 1992a; de Looze et al., 1992b; Desjardins et al., 1998). Other dynamic analyses, such as those used for knee and hip kinematic calculations during gait, depend on the set of BSP data used, both in normal and overweight adults, with differences as large as 60% (Pearsall and Costigan, 1999; Rao et al., 2006). These large differences can negatively impact the ability to predict injury risk, and reflect the need for accurate segment parameter inputs representative of the populations of interest or individuals being studied (Chaffin and Muzaffer, 1991; Marras et al., 1993). Comparisons of predicted parameters can indeed vary by up to 40% due to effects of age, and the specific prediction method used (Durkin and Dowling, 2003). Because predictive methods separately study different population segments, such as normal weight young adults (de Leva, 1996) or older adults (Hughes et al., 2004; Kuczmarski et al., 2000; Pavol et al., 2002), they do not account for the wide ranges of age and body mass index (BMI) in the larger population.

Our previous work has quantified associations of age and BMI with BSPs in American adults (Merrill et al., 2017; Merrill et al., 2019). These associations were statistically and practically significant, and thus justify the need for BSP predictive data sets that reflect the effects of age and obesity. In the current study, the goal is to develop and validate multiple regression predictive models to accurately estimate BSPs by adding individual-level predictors. Thus, we exploited these known age, BMI, and BSP relationships with the inclusion of individual anthropometric measurements. The statistical models were developed and independently validated on a population of American adult workers covering wide age and obesity ranges, and the developed models can be used for calculating representative BSPs in individuals.

2. Methods

The study was approved by the University of Pittsburgh Institutional Review Board. A total of 280 working adults participated. Recruitment was stratified by age group, BMI group and gender in an attempt to represent all sections of the working population. More specifically, working men and women were recruited in approximately equal numbers in four BMI categories (normal weight: $18.5 \leq \text{BMI} < 25.0$, overweight: $25.0 \leq \text{BMI} < 30.0$, obese: $30.0 \leq \text{BMI} < 40.0$, and morbidly obese $\text{BMI} \geq 40.0\ \text{kg m}^{-2}$) across three age groups ($21 \leq \text{age} < 40$), middle ($40 \leq \text{age} < 55$), and old ($55 \leq \text{age} < 70$), such that each of the twenty four gender, age, and BMI subgroups contained approximately the same number of participants.

After obtaining written informed consent, height and mass were measured in order to confirm eligibility based on BMI was confirmed and female participants of child bearing age took a pregnancy test, with a negative result being required for continued participation. Next, approximately 78 anthropometric measurements were collected (Table 1). The segment circumferences were collected with a cloth tape measure, while the segment lengths, widths, and depths were collected with a straight arm anthropometer. Joint width values were collected using a curved arm anthropometer. All of the arm and leg measurements were collected for both body sides. A whole body DXA scan (Hologic QDR

Table 1
Anthropometric measurements collected for use as predictive terms in the BSP models. All arm and leg measurements were performed on left and right sides.

Anthropometric variable	Definition
Waist circumference	Circumference at the umbilicus
Hip circumference	Around largest part of the hip
Upper thigh circumference	Around proximal thigh
Mid-thigh circumference	Around point midway between proximal border of patella and inguinal crease
Lower thigh circumference	Around thigh1 cm above proximal border of patella
Knee circumference	Around medial and lateral femoral epicondyles
Calf circumference	Around largest part of calf
Ankle circumference	Around medial and lateral malleoli
Upper arm circumference	Around midpoint between acromion and olecranon processes
Elbow circumference	Around medial and lateral humeral epicondyles
Lower arm circumference	Around midpoint between lateral humeral epicondyle and ulnar styloid process
Wrist circumference	Around radial and ulnar styloid processes
Hand thickness	Thickness at center of palm
Elbow width	Distance between medial and lateral humeral epicondyles
Wrist width	Between radial and ulnar styloid processes
Knee width	Between medial and lateral epicondyles
Ankle width	Between medial and lateral malleoli
Upper arm length	Lateral humeral epicondyle to acromion
Lower arm length	Ulnar styloid process to lateral humeral epicondyle
Thigh length	Greater trochanter to knee joint center
Shank length	Knee joint center to lateral malleolus
Inter-ASIS distance	Between left and right ASIS
Shoulder level trunk width	Width at shoulder joint center level
Breast level trunk width	Width at nipple level
Mid-breast level trunk width	Width at level midway between nipple and L3-L4
L3-L4 level trunk width	Width at L3-L4 level
Shoulder level trunk depth	Depth at shoulder joint center level
Breast level trunk depth	Depth at nipple level
Mid-breast level trunk depth	Depth at level midway between nipple and L3-L4
L3-L4 level trunk depth	Depth at L3-L4 level
Shoulder level axis depth	Depth from the shoulder joint center/greater trochanter plane to the back at shoulder joint center level
Breast level axis depth	Depth from the shoulder joint center/greater trochanter plane to the back at nipple level
Mid-breast level axis depth	Depth from the shoulder joint center/greater trochanter plane to the back at level midway between nipple level and L3-L4
L3-L4 level axis depth	Depth from the shoulder joint center/greater trochanter plane to the back at L3-L4
C7 height	Distance from ground to C7
Shoulder height	Distance from ground to shoulder joint center
ASIS height	Distance from ground to ASIS
Hip height	Distance from ground to greater trochanter

Fig. 1. Example of a whole body DXA scan prior to division into the segments of interest. The differences in bone, fat, and lean tissue can be visualized based on the individual pixel brightness.

1000/W, Bedford, MA, USA) of each participant was then performed using the same methods used and described in prior studies (Chambers et al., 2010), with the participant lying supine (Fig. 1).

The processing consisted of each scan being split into each major body segment of interest (torso, left and right upper arm, forearm, thigh, and shank), defined using bony landmarks and anatomically defined planes (Chambers et al., 2010), as shown in Fig. 2. Each segment was then split into 3.9 cm tall slices, perpendicular to the long axes of the bones for the arms and legs, and horizontal for the torso, in a similar method to that described by Ganley and Powers (2004). Pixel densities had assumed values of 2.5–3.0 g cm^{-3} for bone, 0.9 g cm^{-3} for fat, and 1.08 g cm^{-3} for lean tissue (Ganley and Powers, 2004). The segment mass, COM and R_G were then calculated from the known slice heights and masses using a custom MATLAB script (Mathworks, Natick, MA, USA). Details regarding the specific parameter calculations from the slice masses are included in Ganley and Powers (2004) and Merrill et al. (2019).

For brevity purposes, all reported data for the forearm, upper arm, thigh, and shank were analyzed on the participants' self-reported dominant side. Segment mass was expressed as percent of the total body mass. COM locations were reported as percent of the segment length from the proximal (superior for the torso) segment border, where a higher value indicates that the COM is located further in the distal (inferior for the torso) direction. The R_G values were also expressed as percent of the segment length, with the R_G location being measured from the calculated COM.

2.1. Statistical analysis

All statistical analyses were stratified due to significant gender differences and complex interactions of gender with age and BMI findings, previously reported by our group (Merrill et al., 2019). For example, males and females demonstrated similar torso BSP parameter trends with varying age and BMI, in contrast to opposite trends in thigh COM location as a function of BMI (Merrill et al., 2019). All fifteen segment parameters of interest (mass, COM, and R_G for the torso, thigh, shank, upper arm, and forearm) were checked for normality, then log transformed as necessary before any further analysis. The full data set of 280 participants was randomly split into two subgroups: the training set, which contained 200 participants, and the testing set, which contained the remaining 80. A multiple regression analysis was performed on the torso, thigh, shank, upper arm, and forearm segment parameters in the training subset with a backward elimination strategy for variable selection and stratified by gender. The initial models contained age, BMI, age and BMI interaction terms, waist, hip, and neck circumferences, and all relevant physical measures taken of the body segment of interest. In each step of the analysis, the predictor with the largest *p*-value was removed, and the analysis was repeated. The process was repeated until the $p < 0.10$ for all remaining predictors. All analyses were performed in JMP Pro 12 (SAS Institute, Cary, NC, USA).

While not direct measurement of all segments, the waist, hip, and neck circumferences were included to all initial models due to their relationship with overall body shape and mass distribution, specifically their ability to define central adiposity, which when included with BMI, can help describe the relative distribu-

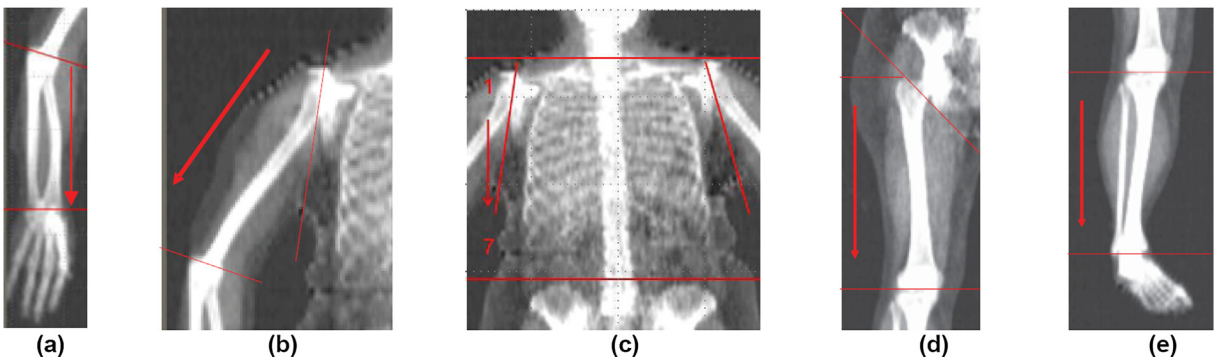

Fig. 2. Segmental boundaries of interest: (a) forearm, (b) upper arm, (c) torso, (d) thigh, (e) shank. During the scan analysis process, each of these segments is separated into a series of 3 pixel (3.9 cm) tall slices, so that the BSPs can be calculated as described by Ganley and Powers (2004) using the known slice mass and height.

tion of mass throughout the torso and appendages within differing degrees of obesity. For example, individuals with more central adiposity will have higher waist and/or hip circumferences than individuals with less central adiposity, meaning that at given BMI, individuals with larger circumferences will have less total and normalized limb mass, along with COM and Rg values more representative of those seen in less obese individuals.

Once the models were finalized, they were used for prediction in the independent validation data set, so that the predicted and actual segment (in-vivo DXA-based) parameters could be compared using the absolute percent error, as well as the root mean square error (RMSE). The total variability explained by the models when applied to the testing set (R^2), along with the improvements of these models (ΔR^2) over previously established models using only age and BMI terms (Merrill et al., 2019) were also reported. Additionally, the actual testing set values were compared to a commonly used segment parameter prediction method (de Leva, 1996) using the same metrics.

3. Results

3.1. Overview

The final study sample consisted of 280 working adults (148 female) ages 21–70 (mean: 44.9 ± 13.4 years). A number of predictors simultaneously remained significant in models for women and men (Tables 2–6), with all but one (upper arm R_G) of the models showing improvement over a previously established method (Merrill et al., 2019) which used only age, BMI, and interaction terms (Table 7). While not all of the models employed the additional anthropometric measures, the majority retained age, BMI, or their interaction terms. The majority of the average prediction errors and normalized RMSE values were within 5% of the actual DXA-based values, while the parameter predictions based on the de Leva (1996) regressions demonstrated higher errors, in some cases up to 60% of the actual measured values (Table 8).

3.2. Torso

The initial torso models included the following variables as potential predictors of the torso BSPs (COM, mass and R_G): age, BMI, their squared and interaction terms in addition to waist, hip, and neck circumference, torso widths, depths, and axis depths (Table 1), and the inter-ASIS distance. The final models, following the stepwise process, identified a number of age- and BMI- related terms among the statistically significant factors, but also various anthropometric predictors (Table 2). When including all identified predictors, the final model explained an average 51% and 74% of the variability in the torso BSPs in female and male participants in the training set, respectively. Including the anthropometric factors explained an additional 13 to 50% of the variability in the torso BSPs above and beyond that explained by the age- and BMI- related terms alone (Table 7). Most importantly, when the final regression models were used to predict the torso BSPs in the test data set, the normalized RMSE values were less than 5%, and the percent prediction errors (relative to the actual in-vivo DXA-based BSPs) were 3% or less. In contrast, the percent prediction errors of the deLeva method ranged between 6% (Torso mass) to 34% (Torso R_G) (Table 8).

3.3. Thigh

The thigh models initially included neck, waist, hip, knee, and three thigh circumferences, taken at the upper, middle, and lower thigh levels (Table 1), as well as knee width and thigh length.

Table 2
Torso center of mass, mass, and radius of gyration multiple regression model estimated coefficients for the final models following the backwards elimination process.

TORSO		Intercept	Age	Age^2	BMI	BMI^2	Age*BMI	$Age*BMI^2$	Age^2*BMI^2	Circumference		Width Level			Depth Level				Inter-ASIS
										Neck	Hip	Shoulder	Breast	Mid breast	L3/L4	Shoulder	Breast	Mid breast	L3/L4	
COM	**M**	57.325	−0.0445	3.09E−04	−0.203	1.56E−03	–	4.64E−05	–	−0.119	–	–	−0.145	0.213	–	−0.149	–	–	0.102	0.105
	F	62.442	–	−2.11E−03	−0.614	9.03E−03	–	–	1.66E−04	2.52E−06	–	0.0567	−0.105	–	–	–	−0.143	–	–	0.099
M	**M**	120.217	−3.831	0.0458	−5.333	0.0842	0.261	−4.16E−03	−3.11E−03	5.02E−05	–	−0.127	–	–	–	−0.536	–	1.050	−0.336	0.266
	F	37.495	–	–	−1.274	9.10E−03	–	–	–	–	–	–	–	–	–	−0.295	0.767	–	0.445	–
Rg	**M**	39.743	−0.417	3.28E−03	−0.546	5.38E−03	0.0177	−1.22E−04	−1.09E−04	–	–	0.0261	–	–	−0.103	0.167	−0.0946	−0.0497	–	–
	F	33.183	−0.0967	–	−0.347	4.72E−03	5.66E−03	−7.65E−05	–	–	–	–	0.0821	–	–	–	–	–	−0.0712	–

Table 3
Thigh center of mass, mass, and radius of gyration multiple regression model estimated coefficients for the final models following the backwards elimination process.

THIGH		Intercept	Age	Age^2	BMI	BMI^2	Age*BMI	Age*BMI^2	Age^2*BMI	Age^2*BMI^2	Circumference						
											Neck	Waist	Hip	Upper thigh	Mid thigh	Lower thigh	Knee
COM	**M**	58.572	−0.438	5.32E−03	−0.264	–	0.0145	–	−1.76E−04	–	−0.107	–	–	–	–	0.227	–
	F	51.351	−0.172	2.08E−03	–	1.24E−03	–	–	–	–	0.111	–	−0.0947	−0.0894	–	0.186	–
M	**M**	11.882	–	−1.63E−04	–	–	–	–	–	–	−0.136	−0.0248	–	0.120	–	–	–
	F	32.272	−1.346	0.0148	−1.955	0.0262	0.0865	−1.29E−03	−9.63E−04	1.45E−05	−0.129	–	–	0.116	0.115	–	0.0927
Rg	**M**	24.421	–	–	–	–	–	–	–	–	0.05	–	−0.0194	−0.0331	−0.0374	–	0.129
	F	29.22	−0.196	0.00213	−0.129	–	0.0061	–	−6.63E−05	–	–	–	–	–	−0.056	–	0.0972

Table 4
Shank center of mass, mass, and radius of gyration multiple regression model estimated coefficients for the final models following the backwards elimination process.

SHANK		Intercept	Age	Age^2	BMI	BMI^2	Age*BMI	Age*BMI^2	Age^2*BMI	Age^2*BMI^2	Shank Length	Circumference					
												Waist	Hip	Knee	Calf	Ankle	Ankle Width
COM	**M**	39.703	–	–	–	–	–	–	–	–	–	–	−0.0341	–	–	–	0.603
	F	46.963	–	−1.87E−03	−0.553	6.75E−03	–	–	1.20E−04	−1.78E−06	−0.110	–	–	−0.238	0.121	0.480	–
M	**M**	3.663	–	−8.45E−05	−0.168	1.00E−03	–	–	–	8.81E−08	–	–	−0.0127	–	0.146	–	–
	F	3.333	−0.0234	–	−0.217	1.32E−03	7.27E−04	–	–	–	–	–	−9.64E−03	–	0.153	0.0508	–
Rg	**M**	32.393	–	−2.19E−03	−0.281	4.82E−03	–	–	1.32E−04	−1.87E−06	0.0372	−0.0132	–	0.0905	−0.183	–	0.170
	F	26.146	–	–	–	4.59E−04	–	–	–	–	–	−0.0111	–	0.0406	−0.150	0.196	–

Table 5
Upper arm center of mass, mass, and radius of gyration multiple regression model estimated coefficients for the final models following the backwards elimination process.

UPPER ARM		Intercept	Age	Age^2	BMI	BMI^2	Age*BMI	Age*BMI^2	Age^2*BMI	Age^2*BMI^2	Upper arm Length	Circumference			
												Waist	Hip	Elbow	Upper Arm
COM	**M**	58.27	−0.229	2.50E−03	–	–	–	–	–	–	–	–	–	–	−0.124
	F	46.182	–	–	–	–	–	–	–	–	–	−0.0575	–	0.337	–
M	**M**	−6.28	0.365	−4.02E−03	0.249	–	−0.0121	–	–	1.33E−04	–	−0.0176	–	0.153	–
	F	2.432	−0.0243	1.07E−04	−0.0346	–	7.55E−04	–	–	–	0.0376	9.97E−03	−0.027	0.0411	0.0527
Rg	**M**	20.405	–	–	−0.122	–	–	–	–	–	–	0.0268	–	0.208	–
	F	35.337	−0.385	4.60E−03	−0.418	3.14E−03	0.0120	–	−1.43E−04	–	–	–	–	–	–

Almost all of the models retained at least one of the age or BMI terms, and all included at least one of the thigh circumference measurements. For thigh COM, upper and lower thigh circumferences were both significant predictors, and both genders had a >20% increase (ΔR^2) in proportion of explained variability (Table 3). Both genders also had similar ΔR^2 for R_G predictions; however, the model for females retained almost all of the age, BMI, and interaction terms, while the male model was solely based on circumference measurements.

When applied to the test data set, the thigh COM and R_G models had normalized RMSE values below 5%, while the mass RMSE was much higher, at 11.6% (Table 8). The thigh R_G mean error was comparable to the torso prediction errors, at about 1.1%; however, the COM and mass predictions were slightly higher, at 3.8 and 7.0%, respectively. All three of the actual thigh parameters had errors of 16–38% when predicted with the deLeva methods (Table 8).

3.4. Shank

The shank prediction models started with neck, waist, hip, knee, calf, and ankle circumferences, as well as knee and ankle widths, and shank length. With the exception of shank COM in males, all of the other parameter predictions included at least one BMI term and calf circumference. In both genders, hip and calf circumferences were included in the final mass models, while waist, knee, and calf circumferences were used in the R_G models.

All of the models other than COM in males showed R^2 increases of over 0.2 (Table 4), with final R^2 values over 0.85 for mass in both genders (Table 7). The predictive power of the anthropometric model for shank COM in males showed a negligible R^2 increase of 0.004 over the previous model using only age and BMI terms. The model only included hip circumference and ankle width, but none of the age terms, or any of the other terms generally associated with obesity, such as BMI or waist or hip circumferences. When applied to the test data set, the COM and R_G predictions were especially accurate, with RMSE under 2.5%, and average errors of all three shank parameters under 5% (Table 8). Predictions by deLeva models had greater error, especially for R_G predictions, with average of over 60%.

3.5. Upper arm

In addition to the age and BMI terms, the upper arm models started with waist, hip, neck, upper arm, and elbow circumferences, and elbow width. The final model for predicting mass in females had an R^2 of about 0.5 (Table 5); however, all of the other models had R^2 of under 0.25. Even though the variance explained by the models approximately doubled for R_G in males and COM in females, the overall values still remained under 15%. The models for mass and R_G in males, and mass and COM in females all included waist and elbow circumferences.

The final model for predicting R_G in females is notable because it did not improve over the previous model, which included all of the age, BMI, quadratic, and interaction terms. None of the anthropometric terms were significant in the final model, and the final R^2 ended up slightly less than the previous model because the non-

Table 6
Forearm center of mass, mass, and radius of gyration multiple regression model estimated coefficients for the final models following the backwards elimination process.

FOREARM		Intercept	Age	Age^2	BMI	BMI^2	Age*BMI	Age^2*BMI	Age*BMI^2	Age^2*BMI^2	Forearm Length	Circumference				
												Waist	Hip	Elbow	Forearm	Wrist
COM	**M**	41.396	−0.0259	1.11E−03	–	3.03E−03	–	–	6.88E−05	–	−0.168	–	–	−0.203	–	0.521
	F	48.113	−0.282	–	−0.529	8.05E−03	0.0177	–	−2.59E−04	–	–	–	−0.377	−0.221	–	0.690
M	**M**	−11.193	0.748	−9.58E−03	0.735	−0.010	−0.0441	6.09E−04	–	5.66E−04	–	−8.26E−03	−0.0145	–	0.0430	0.0897
	F	1.042	–	–	−0.03	3.35E−04	–	–	–	–	0.0214	−3.91E−03	−8.44E−03	0.0460	0.0243	–
Rg	**M**	28.227	−0.0397	4.48E−04	−0.0913	1.40E−03	–	–	–	–	–	–	–	–	−0.0994	0.169
	F	24.706	–	–	−0.0409	–	–	–	–	–	–	0.0160	–	–	−0.144	0.307

significant age, BMI, and interaction terms were removed during the backward elimination process. While the total variance explained by the model was under 20% for R_G for both genders, the RMSE was under 4% when applied to the test data set, with an average error of less than 3% (Table 8). The upper arm COM prediction also had RMSE of less than 5%, while the mass prediction had a higher RMSE of about 10%. The errors of deLeva predictions were again higher, ranging from approximately 17% for COM location, to almost 40% for R_G.

3.6. Forearm

The initial model for the forearm included the age and BMI terms along with waist, hip, neck, forearm, elbow, and wrist circumferences, wrist and elbow widths, and forearm length. All of the final models included at least one of the age or BMI terms, and all except for mass in females included wrist circumference (Table 6). While the mass predictions had the highest R^2 values, they also had larger prediction errors in the test data set, with normalized RMSE of about 9%, and average errors over 7% (Table 8). COM and R_G predictions were more accurate when applied to the test data set, with RMSE under 2.5%, and average errors under 2%. The deLeva parameter predictions forearm mass prediction error was slightly higher than the anthropometric model errors, at a little over 11%; however, the average error in R_G calculation was nearly 60%.

4. Discussion

The new prediction models including individual anthropometric measures in addition to age and BMI terms have increased the accuracy over previous methods which only considered gender (de Leva, 1996), while also having the advantage of simplified requirements for measurement collection compared to other methods dependent on individual body shape (Erdmann and Kowalczyk, 2015; Hatze, 1980). These improvements in accuracy are particularly notable in the torso and thigh segments. The results show that the inclusion of the neck, waist, and hip circumferences are important to include along with BMI for all segment parameter predictions because they provide further insight into how mass is generally distributed throughout the body.

4.1. Torso

The torso parameter predictions in females, particularly COM and R_G, were found dependent not only on age and BMI factors, but also on a number of torso width and depth measurements. While all of the final R^2 values for the female torso predictions are above 0.5, the increases are especially notable for mass and COM predictions (Table 7), indicating that changes in these parameters are highly dependent on the torso geometry of the individual. In contrast to females, the majority of the variation in BSP parameters is explained by age and BMI factors, with anthropometric measurements playing a smaller role in parameter prediction. One finding worth noting among the body measurement effects is that for all three of the male torso BSP variables, shoulder level depth was a highly significant factor ($p < 0.01$), suggesting that the volume of the top of the torso, independent of tissue composition (lean or adipose), plays an important role in predicting these parameters.

4.2. Thigh

In females, the models for thigh COM and R_G retained most of the age and BMI predictors as being significant, suggesting that

Table 7
R^2 values for the final multiple regression models, compared to the values (R_0^2) from the regression models from Merrill (2019), which only account for the associations of the BSPs with age and BMI. The improvements in variation explained by the new models compared to the previously established regressions (ΔR^2) are provided to demonstrate the improvement between the sets of models.

Female	Torso COM	Torso Mass	Torso Rg	Thigh COM	Thigh Mass	Thigh Rg	Shank COM	Shank Mass	Shank Rg	Arm COM	Arm Mass	Arm Rg	Forearm COM	Forearm Mass	Forearm Rg
R^2	0.509	0.633	0.677	0.358	0.663	0.242	0.505	0.861	0.441	0.099	0.503	0.181	0.375	0.672	0.320
R_0^2	0.279	0.138	0.563	0.122	0.163	0.049	0.304	0.174	0.122	0.046	0.197	0.184	0.249	0.272	0.108
ΔR^2	0.230	0.495	0.114	0.236	0.500	0.193	0.201	0.687	0.319	0.053	0.306	−0.003	0.126	0.400	0.212
Male	Torso COM	Torso Mass	Torso Rg	Thigh COM	Thigh Mass	Thigh Rg	Shank COM	Shank Mass	Shank Rg	Arm COM	Arm Mass	Arm Rg	Forearm COM	Forearm Mass	Forearm Rg
R^2	0.635	0.660	0.739	0.387	0.558	0.570	0.209	0.853	0.622	0.131	0.218	0.133	0.338	0.446	0.400
R_0^2	0.506	0.453	0.573	0.107	0.440	0.292	0.205	0.502	0.253	0.114	0.180	0.062	0.174	0.352	0.245
ΔR^2	0.129	0.207	0.166	0.280	0.118	0.278	0.004	0.351	0.369	0.017	0.038	0.071	0.164	0.094	0.155

Table 8
Root mean square error (RMSE) for the model predictions expressed as a percentage of the actual measured values in the test data set, and their comparison to those of de Leva (1996). The RMSE functions as a measure of predictive ability of the final models, while the percentage differences serve to demonstrate the relative differences in the BSP terms, as they would be applied to biomechanical models.

	Torso			Thigh			Shank			Arm			Forearm		
	COM	Mass	Rg	COM	Mass	Rg	COM	Mass	Rg	COM	Mass	Rg	COM	Mass	Rg
RMSE	1.675	5.241	1.596	4.812	10.951	1.665	2.408	5.681	1.468	4.623	10.032	3.374	2.122	9.030	1.432
Diff (predicted)	1.34	4.35	1.25	3.01	6.17	1.23	1.98	4.46	1.15	3.63	7.48	2.68	1.57	6.81	0.88
Diff (deLeva)	19.65	6.36	33.94	16.85	27.09	38.78	9.66	15.02	62.81	16.83	26.22	39.67	9.84	11.60	59.82

while individual thigh anthropometry explains most of the variation in thigh mass ($\Delta R^2 = 0.49$), age and obesity status explain the distribution of mass within the thigh. In males, most of the age and BMI factors are significant in COM prediction, while thigh mass and R_G predictions are almost entirely dependent on circumference measurements. The thigh R_G prediction in males is entirely dependent on circumference measurements (neck, hip, knee, and upper and mid-thigh), and does not include any of the initial age or BMI predictors, indicating that this parameter is only dependent on the shape of the individual, and independent of age or obesity status.

4.3. Shank

With the exception of shank COM prediction in males, all of the prediction models included calf circumference. The calf circumference measurement is notable because it is defined as the largest measurement around the calf, as opposed to other measurements, which are defined relative to anatomical landmarks. The calf circumference is a highly significant predictor ($p < 0.001$) for shank mass in both genders because it is proportional to the maximum cross section of the shank, instead of being in a predefined location. Similarly to the thigh R_G in males, the COM value in males is also only predicted by anthropometric measurements, meaning that this value is also independent of age and obesity status.

4.4. Upper arm and forearm

Including individual anthropometric measurements in the prediction of the upper extremity's BSPs variables had varying and complex effects. For example, while the female upper arm COM prediction model was dependent only on individual geometry, in males, this BSP variable was dependent both on age and individual anthropometry data. The forearm BSP predictions were highly dependent on individual anthropometric measures, in addition to age and BMI terms, in both males and females.

Overall, nearly all of the observed statistical models benefitted from including individual anthropometric measurements. In addition to observing the effects of age and BMI, data points such as waist and hip circumference provide additional measures of obesity, and whole body mass distribution. By using separate randomly selected training and test data sets, this study was able to develop and validate anthropometry based prediction models for the segment parameters of interest. The independent validation is imperative in such settings to assess true model performance, and not an overly optimistic metric attainable due to over fitting. These anthropometric models were able to predict the parameters more precisely than previous modeling methods (de Leva, 1996).

5. Conclusion

In summary, the findings of the present study provide statistical tools that allow the prediction of BSPs using simple individual characteristics such as age, BMI and body measurements. The final models presented have shown large improvements over the de Leva (1996) and Merrill et al (2019) models, particularly in the torso and thigh segments. It is important to note that the previous work using this same data set (Merrill et al., 2019) examined the relationships of age and BMI with these segment parameters, however the final models were not predictive in nature, and not intended to be used as such. By comparison, the results of this study are intended to be used to predict BSPs for individuals.

Compared to the method explained by Erdmann and Kowalczyk (2015), this method consists of fewer torso measurements to predict the torso BSPs, whereas as Erdmann and Kowalczyk divided the torso into several functional segments, accomplishing their goal of providing a more detailed tissue distribution description. When comparing these results to those of Hatze (1980), these final models and predictive abilities are again far simpler, both mathematically and in practice for data collection and parameter prediction.

Limitations of this study involve the study population, which consisted only of healthy American working aged adults with full time jobs. Factors such as activity levels and overall fitness were not considered, and would likely impact body mass distribution. While ethnicity was not taken into account in the statistical analysis, the participants recruited reflected the diversity of the American working population, and the use of the multiple

anthropometric measurements accounted for differences in whole body and segment shaped in a more detailed manner than including ethnicity as a single predictor.

Because the DXA scans were collected only in the frontal plane, with the participants lying supine, some degree of weight shifting may have occurred, which would not be present during standing. Additionally, the specific segment definition used for the torso was chosen for its applicability to inverse dynamics calculations and individual variability (Merrill et al., 2018), and may not be directly comparable to other methods of trunk segment parameter calculations. While only frontal plane data were employed, previous work comparing parameters in obese and non-obese adults has noted errors of less than 0.1% of the segment length when estimating sagittal plane R_G values using frontal plane values (Fang et al., 2017).

For the purpose of brevity, only the dominant side arm and leg segment parameters were analyzed. Only observing the dominant side has the most relevance for performing many occupational tasks and sports activities, and symmetry may be assumed for other tasks.

Finally, our sample size may not be as large as it appears at the first glance, considering the large numbers of independent variables that we considered in the models. We could have examined more complex models had we recruited an even larger number of participants. Thus, the prediction equations we were able to formulate and improvements elicited should be considered preliminary, needing further refinement and validation. Despite the limitations, we feel the many strengths of our study outweigh them in investigating the complex associations between anthropometrics and body segment parameters, and exploiting the same for more accurate prediction of the latter.

Declaration of Competing Interest

The authors have no financial interests in relation to the work described in this research manuscript.

Acknowledgements

CDC/NIOSH- R01-OH010106, “Obesity and Body Segment Parameters in Working Adults.”

NIH/NIA-P30-AG024827, “The Pittsburgh Claude D. Pepper Older Americans Independence Center.”

References

Chaffin, D.B., Andersson, G.B.J., Martin, B.J., 2006. Occupational Biomechanics. Wiley-Interscience, Hoboken, New Jersey.

Chaffin, D.B., Muzaffer, E., 1991. Three-dimensional biomechanical Static Strength Prediction Model sensitivity to postural and anthropometric inaccuracies. IEEE Trans. 23, 215–227.

Chambers, A.J., Sukits, A.L., McCrory, J.L., Cham, R., 2010. The effect of obesity and gender on body segment parameters in older adults. Clin. Biomech. 25, 131–136.

Chandler, R.F., Clauser, C.E., McConville, J.T., Reynolds, H.M., Young, J.W., 1975. Investigation of inertial properties of the human body. U.S. Department of Transportation, Washington, DC DOT HS-801 430/AMRL-TR-74-137.

Chen, S.-C., Hsieh, H.-J., Lu, T.-W., Tseng, C.-H., 2011. A method for estimating subject-specific body segment inertial parameters in human movement analysis. Gait Posture 33, 695–700.

Damavandi, M., Farahpour, N., Allard, P., 2009. Determination of body segment masses and centers of mass using a force plate method in individuals of different morphology. Med. Eng. Phys. 31, 1187–1194.

de Leva, P., 1996. Adjustments to Zatsiorsky-Seluyanov’s segment inertia parameters. J. Biomech. 29, 1223–1230.

de Looze, M.P., Kingma, I., Bussmann, J.B., Toussaint, H.M., 1992a. Validation of a dynamic linked segment model to calculate joint moments in lifting. Clin. Biomech. 7, 161–169.

de Looze, M.P., Bussmann, J.B., Kingma, I., Toussaint, H.M., 1992b. Different methods to estimate total power and its components during lifting. J. Biomech. 25, 1089–1095.

Dempster, W.T., 1955. Space requirements of the seated operator. Wright Air Development Center, Wright Patterson Air Force Base, Ohio WADC-TR-55-159.

Desjardins, P., Plamondon, A., Gagnon, M., 1998. Sensitivity analysis of segment models to estimate the net reaction moments at the L5/S1 joint in lifting. Med. Eng. Phys. 20, 153–158.

Durkin, J.L., Dowling, J.J., 2003. Analysis of body segment parameter differences between four human populations and the estimation errors of four popular mathematical models. J. Biomech. Eng. 125, 515–522.

Erdmann, W.S., Kowalczyk, R., 2015. A personalized method for estimating centre of mass location of the whole body based on differentiation of tissues of a multi-divided trunk. J. Biomech. 48, 65–72.

Fang, Y., Morse, L.R., Nguyen, N., Tsantes, N.G., Troy, K.L., 2017. Anthropometric and biomechanical characteristics of body segments in persons with spinal cord injury. J. Biomech. 55, 11–17.

Ganley, K.J., Powers, C.M., 2004. Anthropometric parameters in children: a comparison of values obtained from dual energy x-ray absorptiometry and cadaver-based estimates. Gait Posture 19, 133–140.

Hansen, C., Venture, G., Rezzoug, N., Gorce, P., Isableu, B., 2014. An individual and dynamic body segment inertial parameter validation method using ground reaction forces. J. Biomech. 47, 1577–1581.

Hatze, H., 1980. A mathematical model for the computational determination of parameter values of anthropometric segments. J. Biomech. 13, 833–843.

Hughes, V.A., Roubenoff, R., Wood, M., Frontera, W.R., Evans, W.J., Fiatarone Singh, M.A., 2004. Anthropometric assessment of 10-y changes in body composition in the elderly. Am. J. Clin. Nutr. 80 (2), 475–482.

Jensen, R.K., 1978. Estimation of the biomechanical properties of three body types using a photogrammetric method. J. Biomech. 11, 349–358.

Kuczmarski, M.F., Kuczmarski, R.J., Najjar, M., 2000. Descriptive anthropometric reference data for older Americans. J. Am. Diet. Assoc. 100, 59–66.

Marras, W.S., Lavender, S.A., Leurgans, S.E., Rajulu, S.L., Allread, W.G., Fathallah, F.A., Ferguson, S.A., 1993. The role of dynamic three-dimensional trunk motion in occupationally-related low back disorders. Spine 18 (5), 617–628.

Merrill, Z., Bova, G., Chambers, A.J., Cham, R., 2018. Effect of trunk segment boundary definitions on frontal plane segment inertia calculations. J. Appl. Biomech. 34 (3), 232–235.

Merrill, Z., Chambers, A.J., Cham, R., 2017. Impact of age and body mass index on anthropometry in working adults. In: Proceedings of the Human Factors and Ergonomics Society Annual Meeting, vol. 61, No. 1, pp. 1341–1345.

Merrill, Z., Perera, S., Chambers, A.J., Cham, R., 2019. Age and body mass index associations with body segment parameters. J. Biomech. 88, 38–47.

Pavol, M.J., Owings, T.M., Grabiner, M.D., 2002. Body segment inertial parameter estimation for the general population of older adults. J. Biomech. 35, 707–712.

Pearsall, D.J., Costigan, P.A., 1999. The effect of segment parameter error on gait analysis results. Gait Posture 9, 173–183.

Rao, G., Amarantini, D., Berton, E., Favier, D., 2006. Influence of body segments’ parameters estimation models on inverse dynamics solutions during gait. J. Biomech. 39, 1531–1536.

Sanders, R.H., Chiu, C.-Y., Gonjo, T., Thow, J., Oliviera, N., Psycharakis, S.G., Payton, C. J., McCabe, C.B., 2015. Reliability of the elliptical zone method of estimating body segment parameters of swimmers. J. Sports Sci. Med. 14, 215–224.